ISSN 1 746-7233, England, UK
World Journal of Modelling and Simulation
Vol. 6 (2010) No. 4, pp. 310-320

Steady state analysis of a wind driven single-phase SEIG using particle swarm optimization

J. Upendar*, G. K. Singh, C. P. Gupta

Department of Electrical Engineering, Indian Institute of Technology, Roorkee 247667, India

(*Received July 31 2009, Accepted May 1 2010*)

Abstract. This paper presents the steady state analysis of a wind driven single phase single winding self excited induction generator (SEIG) with and without shunt compensation. The performance equations are derived using loop impedance method and graph theory. This reduces the heavy computation work of segregating real and imaginary components of complex impedance of induction generator (IG) for deriving the specific models for each operating models (short-shunt and long-shunt, etc.). Steady state analysis of single phase SEIG is predicted by solving the equations developed by graph theory with the help of PSO. The system performance is studied considering the excitation voltage, frequency and speed of rotation of the driving machine. The feasibility of the new algorithm is demonstrated by the numerical example and results show the competitiveness of the PSO. Computed results are compared with the results obtained by Newton-Raphson method to verify the feasibility of the developed algorithm.

Keywords: particle swarm optimization, SEIG, self-excitation, short/long shunt compensation

1 Introduction

The optimal utilization of available natural energy is noticed as a new energy source which replaces conventional energy source. The power generation by natural energy such as solar energy, bio gas, wind force, wave force are proposed to decreases the global warming and environmental detritions due to use of conventional fossil fuels for the generation of power. It is preferred to use suitable stand-alone energy sources which are locally available.

The SEIG applied to conventional wind power generation has many advantageous and features such as brushless ness and rugged construction, low cost, maintenance and operational simplicity, soft-protection against faults, no need of separate DC excitation scheme, good dynamic response and capability to generate power at varying speeds of the prime mover. With these advantages SEIG can be operated standalone/isolated mode or in parallel with synchronous generator for remote and rural area electrification and in grid mode. Therefore the study of SEIG has regained importance and hence this paper deals with new methods for the steady state analysis of single phase SEIG with and without compensation.

Many investigations by several authors[1, 2, 4, 6–9], on suitability exploration, and various optimization and non-optimization technique for the accurate analysis of SEIG have been made. Most of the analyses[1, 6, 8] are based on Newton-Raphson (NR) method which contains the real and imaginary components that are non-linear in nature and X_c, X_M and frequency (F), voltage magnitude as variables. Chen[2] used the pattern search method of Hooke and Jeeves method for the determination of per unit frequency and magnetizing reactance in analyzing single phase SEIG using 3-phase machine. Velusami and Singervelu[9] have proposed a Fuzzy logic based analysis of SEIG to compute unknown values. This method requires the prior knowledge of membership functions and fuzzy rules, which is difficulty to program separately for different applications and also in case of high number of fuzzy rules in system.

* Corresponding author. Tel.: +91-9410109968. *E-mail address*: jallaupendar@gmail.com.

Recently, PSO[3, 5] has emerged as powerful and robust tool for solving the linear, non-linear and differential equations. The main advantage PSO is that, this method does not requires calculation of initial values or inverses of matrix, which generally affects the effectiveness of some of optimizations methods. However as a robust optimization technique, the application of PSO in analyzing the modeling the SEIG have not been reported till now.

Therefore, in this paper, the system equations for steady state analysis are formulated using branch-impedance analysis of SEIG equivalent circuit. The resulting single equation is solved using PSO method, which minimizes the tedious mathematical calculations.

To investigate the single phase SEIG configuration, both capacitor and load are connected across the main winding. A MATLAB based program has been developed to implement the proposed method. A comparative study of the results obtained with PSO method and NR method is also carried out to verify the occurrence of proposed method analysis. It is observed that, the computation time per iteration and computation time for convergence of fitness function are very less compared with the solution using NR method.

2 System modeling using graph theory

The prototype of wind driven single phase single winding self excited induction generator (SEIG) with and without shunt compensation is given in Fig. 1 (a), (b), (c), which is driven by the turbine. The steady state equivalent circuit of the SEIG including short-shunt and long-shunt excitation is as shown in Fig. 2. The equivalent circuit is valid for all types of speeds(v).

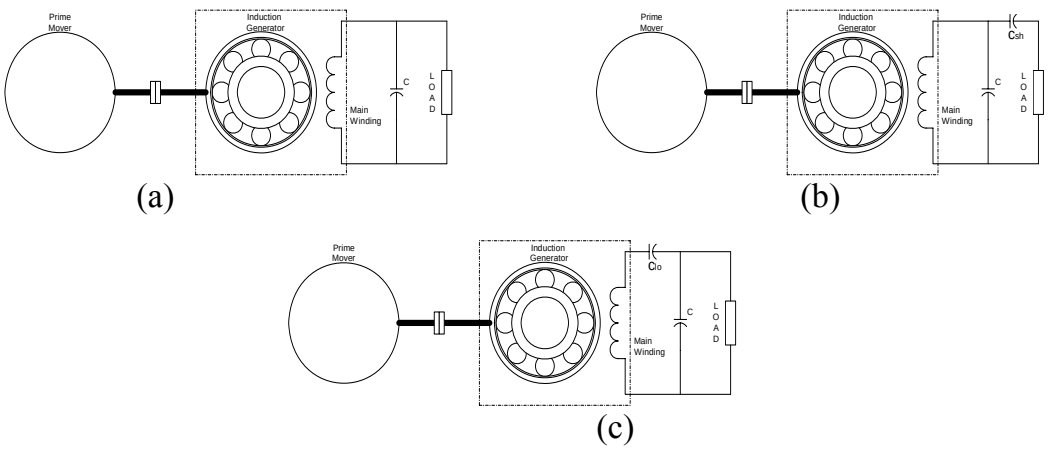

Fig. 1. Block diagram of single-phase single winding SEIG (a) simple-shunt, (b) short-shunt and (c) long-shunt

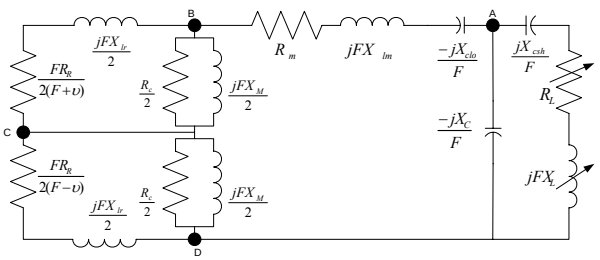

Fig. 2. Steady state equivalent circuit of SEIG with short/long shunt excitation

For analysis, the different values of circuit parameters are defined as:

$$Z_1 = \frac{R_c}{2},\ Z_2 = \frac{jFX_M}{2},\ Z_3 = \frac{R_c}{2},\ Z_4 = \frac{jFX_M}{2},\ Z_5 = R_m + jFX_M - \frac{jX_{\text{clo}}}{F},\ Z_6 = \frac{-jX_c}{F},$$
$$Z_7 = \frac{FR_R}{2(F+v)} + \frac{jFX_{lr}}{2},\ Z_8 = \frac{FR_R}{2(F-v)} + \frac{jFX_{lr}}{2},\ Z_9 = R_L + jFX_L - \frac{jX_{\text{csh}}}{F}.$$

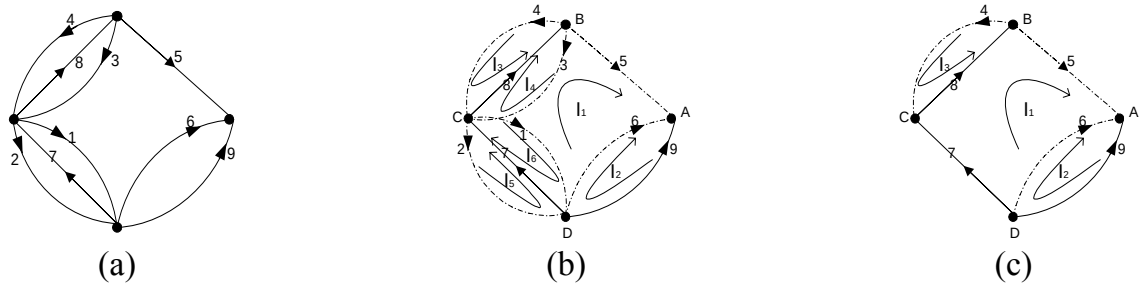

Fig. 3. Equivalent (a) graph (b) tie-set and (c) reduced tie-set of SEIG

Thus there exists at least one path along branches between every pair of nodes of a graph. The equivalent circuit of SEIG is replaced with equivalent graph as shown in Fig. 3 (a). In constructing graph of a network, an ideal voltage source is replaced by a short circuit (shorted branch), and current source is replaced by an open circuit element (open branch). The tie-set for the equivalent graph is as shown in Fig. 3 (b) which contains 3 branches (elements 7, 8, 9), where as link (elements 1, 2, 3, 4, 5 and 6) corresponds a fundamental loop. The direction of loop is assumed as same orientation of its defined link. The equilibrium equation in matrix form on the basis of loop (Tie-set) analysis is represented as Eq. (1).

$$[BZ_bB^T][I_L] = [B][Z_bI_s - V_s]. \tag{1}$$

Since there are no voltage sources and current sources in the Fig. 2. $[\boldsymbol{V}_s]$, $[\boldsymbol{I}_s]$ becomes zero. Thus above equilibrium equation becomes as Eq. (2).

$$[\boldsymbol{B}\boldsymbol{Z}_b\boldsymbol{B}^T][\boldsymbol{I}_L] = 0, \tag{2}$$

where, $\boldsymbol{Z}_b = \text{diag}\{z_1, z_2, \cdots, z_9\}$, $\boldsymbol{I}_L = [I_{L1}, I_{L2}, I_{L3}]^T$ and $\boldsymbol{B}$ =Tie-set matrix of Fig. 3 (b) as shown in Tab. 1.

Table 1. Tie-set matrix of Fig. 3 (b)

Loop currents	Branches								
	1	2	3	4	5	6	7	8	9
I_{L1}	0	0	0	0	1	0	1	1	-1
I_{L2}	0	0	0	0	0	1	0	0	-1
I_{L3}	0	0	0	1	0	0	0	1	0
I_{L4}	0	0	1	0	0	0	0	1	0
I_{L5}	0	1	0	0	0	0	1	0	0
I_{L6}	1	0	0	0	0	0	1	0	0

Here, number of rows equal to number of loops and number of columns equal to the number of branches present in the Tie-set. After substituting matrix $\boldsymbol{B}$, Eq. (2) becomes

$$\begin{bmatrix} z_5+z_7+z_8+z_9 & z_9 & z_8 & z_8 & z_7 & z_7 \\ z_9 & z_6+z_9 & 0 & 0 & 0 & 0 \\ z_8 & 0 & z_4+z_8 & z_8 & 0 & 0 \\ z_8 & 0 & z_8 & z_3+z_8 & 0 & 0 \\ z_7 & 0 & 0 & 0 & z_2+z_7 & z_7 \\ z_7 & 0 & 0 & 0 & z_7 & z-2+z_7 \end{bmatrix} \begin{bmatrix} I_{L1} \\ I_{L2} \\ I_{L3} \\ I_{L4} \\ I_{L5} \\ I_{L6} \end{bmatrix} = 0. \tag{3}$$

The above equation can be assumed as:

$$[\boldsymbol{T}][\boldsymbol{I}_L] = 0, \tag{4}$$

where $[\boldsymbol{T}] = [\boldsymbol{B}\boldsymbol{Z}_b\boldsymbol{B}^T]$.

For the steady state analysis of the single phase single winding SEIG, the core losses of R_c of both the forward and backward fields and also magnetization of '$-ve$' sequence rotor circuit are neglected. After removing the elements z_1, z_2, z_3, from the Fig. 3 (a) the corresponding tie-set can be represented as 3 (c) Then the tie-set matrix ($\boldsymbol{B}$) for the reduced graph becomes as in Tab. 2. Thus, the Eq. (2) can be computed from the

Table 2. Tie-set matrix of Fig. 3 (c)

Loop currents	Branches					
	4	5	6	7	8	9
I_{L1}	0	1	0	1	1	-1
I_{L2}	0	0	1	0	0	-1
I_{L3}	1	0	0	0	1	0

matrix $[\boldsymbol{T}]$ of the reduced Tie-set as:

$$\begin{bmatrix} z_4+z_9 & z_8 & 0 \\ z_8 & z_5+z_7+z_8+z_9 & z_9 \\ 0 & z_9 & z_6+z_9 \end{bmatrix} \begin{bmatrix} I_{L1} \\ I_{L2} \\ I_{L3} \end{bmatrix} = 0. \tag{5}$$

Parameters X_{clo} and X_{csh} can be substituted in z_5 and z_9 according to the compensation used.

Under steady state self excitation operation, IL cannot be equal to zero. Therefore from Eq. (4), $[\boldsymbol{T}]$ is equal to zero and it should be singular. Since matrix $[\boldsymbol{T}]$ is a complex quantity.

$$\|\boldsymbol{T}\| = 0 \;\text{ i.e }\; \sqrt{(\text{real}\|\boldsymbol{T}\|)^2 + (\text{imag}\|\boldsymbol{T}\|)^2}, \tag{6}$$

where $\|\boldsymbol{T}\|$ is the determinant of matrix $[\boldsymbol{T}]$, which is a complex quantity.

To solve the above Eq. (6), a PSO based approach is used as which can be explained in the section 3 and 4.

3 Particle swarm optimization

Particle swarm optimization is a population-based optimization technique developed by Kennedy and Eberhart[3, 5]. It is initialized with a population of random solutions. The algorithm searches for optima satisfying some performance index over generation. It uses the number of agents (particles) that constitutes a swarm moving around in the search space looking for best solution. The PSO technique can generate high quality of optimization solution within a short computation time and exhibits a more stable convergence characteristic than other optimization methods.

The PSO contains "s" individual swarms called particles. Each particle represents a possible solution to a problem with d-parameters represent velocity components. These parameters move with an adaptable velocity within the search space and retain its own memory with the best position it ever reached. The parameters get changed when moving from present iteration to the next iteration. At every iteration, the fitness function as a quality measure is calculated by using its position vector. Each particle keeps track of its own position, which is associated with the best fitness it has achieved so far. The best position obtained so far for particle i keeps the track as $\boldsymbol{P}^i_{\text{best}} = (P^{i1}_{\text{best}}, P^{i2}_{\text{best}}, P^{i3}_{\text{best}}, \cdots, P^{id}_{\text{best}})$. The best global version particle among the entire group of particles keeps the track of G_{best}.

Velocity for particle i, at iteration $t+1$ can be updated using velocity contained in previous iteration t, to be represented as

$$\vec{V}_{id}(t+1) = w \cdot \vec{V}_{id}(t) + c_1\varphi_1(P^{id}_{\text{best}} - P_{id}(t)) + c_2\varphi_2(G^{id}_{\text{best}} - P_{id}(t)), \tag{7}$$

where, $i = 1, 2, 3, \cdots, s$; $d = 1, 2, 3, \cdots, m$; m =number of input variables to be optimized. One set of all input variables is called as one particle. s =number of particles in a group; w = inertia weight factor, varies linearly from $w_{\min}$ to $w_{\max}$, ranges between $(0, 1)$; c_1, c_2 = cognitive and social acceleration factors respectively; φ_1, φ_2 =uniformly distributed random numbers in the range of $(0, 1)$. $P_{id}(t)$ = current position of i^{th} particle, of input variable d at iteration t.

Updated velocity must be within the specified range. If it violates the limits, it is set to a popular value. The velocity change of PSO in Eq. (7) consists of three parts. The first part is the momentum part, which prevents the velocity to be changed abruptly. The second part is the cognitive part, which represents the private thinking of itself, means learning from its own flying experience. The third part is the social part, which represents the collaboration among the particles learning from the group best flying experience. The balance among these three parts determines the balance of global and local search ability, therefore, the performance of PSO.

Then the new position of each particle is evaluated as sum of its previous position and corresponding updated velocity obtained in Eq. (7), can be represented as

$$\vec{P}_{id}(t+1) = \vec{P}_{id}(t) + \vec{V}_{id}(t+1). \tag{8}$$

These operations are repeated for a predefined number of iterations or until fitness is reached. Computational process of the proposed algorithm is shown in Fig. 4.

4 Problem formulation of objective function and its implementation

A PSO based computational procedure as illustrated in Fig. 4 is used to optimize the X_M and F parameters of Eq. (6) The main structure of proposed algorithm contains the evaluation of P_{best}, G_{best}, updating of velocity particles for each particle position in every iteration, until the fitness function f becomes below tolerance $(\varepsilon = 0)$ value.

$$\min\ f(X_M, F) = \min\ (\ \sqrt{(\text{real}\|\boldsymbol{T}\|)^2 + (\text{imag}\|\boldsymbol{T}\|)^2}). \tag{9}$$

The following subsections discuss the main computational process of the proposed algorithm:

Step 1. Setup the PSO parameters such as s, c_1, c_2, $\varphi_(1)$, $\varphi_(2)$, w etc. In our implementation, the inertia weight w is linearly decreasing from 0.9 to 0.4, c_1 and c_2 are selected as 2, number of particles considered as $s = 25$.

Step 2. Create the individual initial particles and velocity particles randomly as,

$$[(X_{M1}, X_{M2}, \cdots, X_{Mi}), (V^{X_{M1}}, V^{X_{M2}}, \cdots, V^{X_{Mi}})],$$
$$[(F_1, F_2, \cdots, F_{Mi}), (V^{F_1}, V^{F_2}, \cdots, V^{F_i})].$$

The each iteration is composed of '$2.d.s$' components respectively.

Step 3. To evaluate the quality of solution, the fitness function f has been calculated for each individual as given in Eq. (9).

Step 4. Update the P_{best} of parameters X_m and F for each individual, also update the G_{best}. For each individual, if the current solution is better than P_{best}, then replace the P_{best} by the current. Finally, if the fitness of any particle is better than G_{best}, and then replace the G_{best}. In first iteration, the current value of individuals and P_{best} both are same.

Step 5. Checks the end condition, if it reached, then stop the algorithm. In this study, the end conditions of PSO are

(i) G_{best} should be below tolerance value 'ε'.

(ii) The maximum number of iterations reached.Otherwise, move to the next step.

Step 6. Update the velocity and position particles separately. Where the new values of velocity and position particles for the next iteration are calculated as follows:

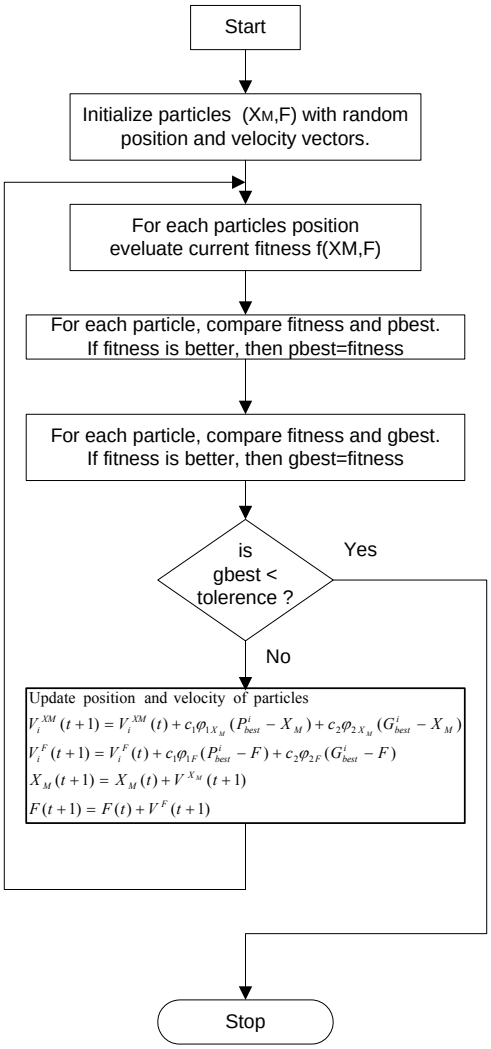

Fig. 4. Flowchart for the PSO algorithm

$$V^{X_{Mi}}(t+1) = V^{X_{Mi}}(t) + C_1\varphi_{1X_M}(P^i_{\text{best}} - X_M) + C_2\varphi_{2X_M}(P^i_{\text{best}} - X_M), \tag{10}$$

$$V_i^F(t+1) = V_i^F(t) + C_1\varphi_{1F}(P^i_{\text{best}} - F) + C_2\varphi_{2F}(P^i_{\text{best}} - F). \tag{11}$$

The left side values of above equations are taken from present iteration of corresponding particle position and parameters. The particle positions are updated using the equations:

$$X_M(t+1) = X_M(t) + V^{X_M}(t+1), \quad F(t+1) = F(t) + V^F(t+1). \tag{12}$$

Then, repeat the steps 3-5 till the end condition is reached.

The simple computer algorithm is developed to incorporate the above procedure, thus, the steady state values of the X_M, F are computed for any given values of speed, capacitance (C), Load (R_L).The air-gap voltage V_g/F is calculated using the parameters (X_M, F) obtained from proposed PSO algorithm. Using these parameters the study state performance of the equivalent circuit can be studied. To get the steady state performance, similar procedure is followed, for the other case , with X_C, F as unknown parameters to maintain the required voltage at terminals of machine for varying loads and speeds.

5 Results and discussion

The performance of 0.75 KW, 4-pole SEIG (Appendix) has been investigated with the proposed model developed using graph theory and PSO. The machine parameters of equivalent circuit discussed in paper[4, 9]

have been considered for detailed investigation of analysis and compared the results with the Newton-Raphson method.

5.1 Without compensation

At no-load, the characteristics of the variation of the excitation capacitance at various speeds were studied as shown in Fig. 5. Fig. 6 presents the characteristics of stator produced voltage V_t of the SEIG, during the variation of speed of the prime mover, at varying excitation capacitances, which buildup the voltage successfully during the different conditions.

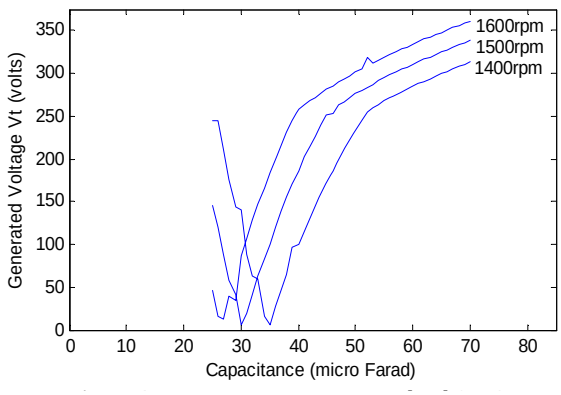

Fig. 5. Capacitance versus V_t at no-load SEIG

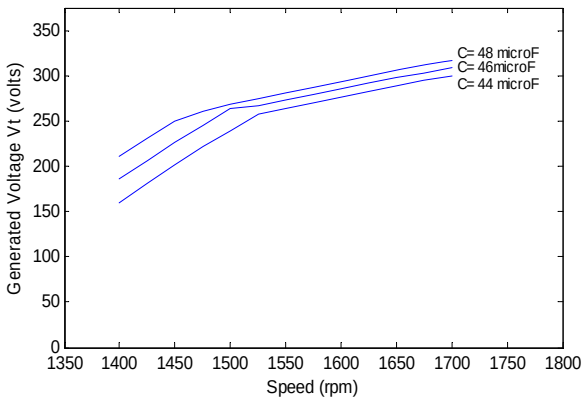

Fig. 6. Speed versus V_t at no-load SEIG

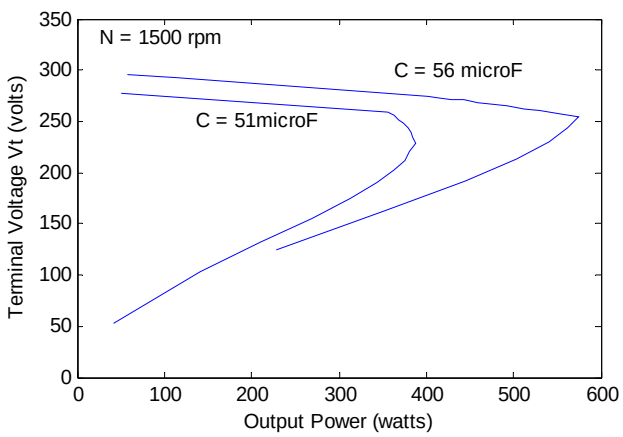

Fig. 7. V_t characteristics at u.p.f load

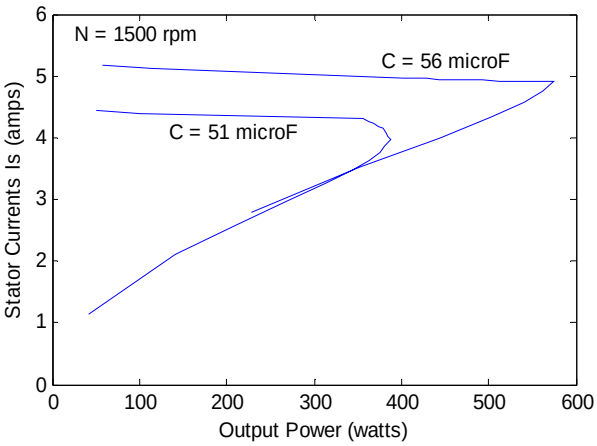

Fig. 8. Is characteristics at u.p.f load

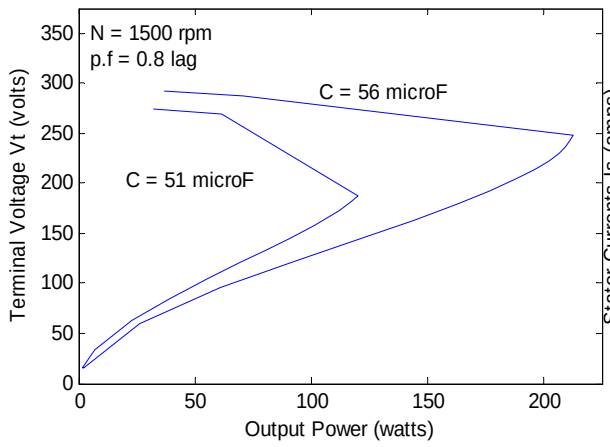

Fig. 9. V_t characteristics at 0.8 p.f load

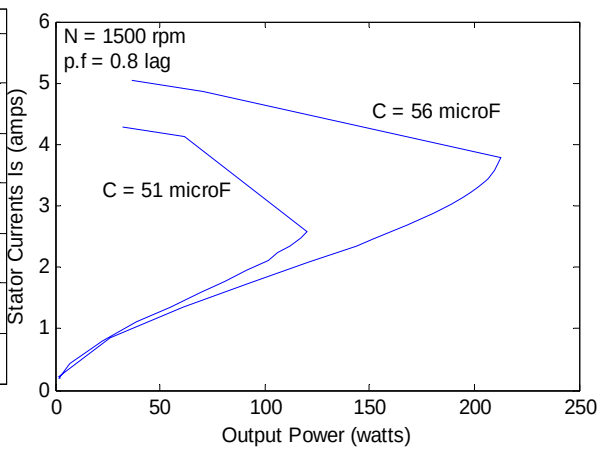

Fig. 10. Is characteristics at 0.8 p.f load

From Figs. 5 and 6, it is observed that the capacitance and speed should be maintained above some threshold value, to the successful voltage buildup.

For upf-load on SEIG, the variation of terminal voltage and variation of stator current (I_s) with output power were studied when the rotor is driven at synchronous speed for two values of excitation capacitances and results obtained are shown in Figs. 7 and 8. For 0.8 pf load on SEIG, the variation of terminal voltage (Vt) and stator current (I_s) are shown in Figs. 9 and 10, respectively with different excitation capacitances and driven at synchronous speed. This has given the poor voltage regulation as exciting capacitance decreases, because of reactive power consumption by reactive load and magnetizing volt ampere of generator.

5.2 Capacitance calculation to maintain the rated terminal voltage

From Fig. 7 and Fig. 9 it is observed that, the terminal voltage decreases under load condition even for fixed values of excitation capacitances and speed. This is overcome by increasing the excitation capacitances as load is increased as depicted in Fig. 11. The computed values of g_c for different loads at constant terminal voltage and at various speeds are plotted in Fig. 11. For calculating these capacitances to maintain the constant terminal voltage, the similar PSO algorithm discussed in section III and IV is implemented by assuming the X_C, F as unknown parameters with the fitness function as

5.3 With short-shunt compensation

To improve the voltage regulation and to avoid the loss of excitation after the load connection, short shunt compensated SEIG is studied with the upf and 0.9 pf lagging loads as shown in Figs. 15, 16, 17 and 18. In short-shunt connection, long-shunt component X_{clo}/F is not presents in z_5. It is observed that, due to addition of the short-shunt component, it enables almost constant voltage across load at constant speed operation, regardless of the load values. No attempts were made to get the optimum values of capacitances. Capacitance $C_{sh} = 65\ \mu F$ and excitation capacitance $C = 42.37\ \mu F$ are used for excitation and compensation purpose. To find the unknown quantities X_M and F with short-shunt compensation, the Eq. (9) is solved with proposed PSO algorithm by including X_{csh} in z_9.

During 0.9 pf load operation, large drooping in the load voltage and terminal voltage at certain loads is observed.

Table 3. Comparision of proposed method with NR method

S.no	Load (RL)	Proposed PSO method		NR method	
		X_M (in $p.u$)	F (in $p.u$)	X_M (in $p.u$)	F (in $p.u$)
1	40	2.589348	0.994847	2.589370	0.994849
2	20	2.624103	0.993059	2.624409	0.993046
3	5	2.895632	0.982824	2.895658	0.982824
4	4.8	2.913673	0.982283	2.914160	0.982285
5	4.6	2.934706	0.981702	2.934735	0.981702
6	4.4	2.957706	0.981070	2.957732	0.981070
7	4.2	2.983579	0.980383	2.983610	0.980384
8	4.0	3.013255	0.979631	3.012919	0.949632
9	3.8	3.046353	0.978809	3.046382	0.978810
10	3.6	3.084876	0.977900	3.084925	0.977905
11	3.4	3.129768	0.976907	3.129760	0.976901
12	3.2	3.182656	0.975785	3.182520	0.975785
13	3.0	3.245601	0.974540	3.245449	0.974539
14	2.8	3.321659	0.973132	3.321699	0.973132
15	2.6	3.416437	0.971530	3.415859	0.971538
16	2.4	3.534799	0.969732	3.534847	0.969714
17	2.2	3.689566	0.967606	3.689611	0.967607
18	2.0	3.898439	0.965145	3.898498	0.965146
19	1.8	4.194738	0.962235	4.194733	0.962237

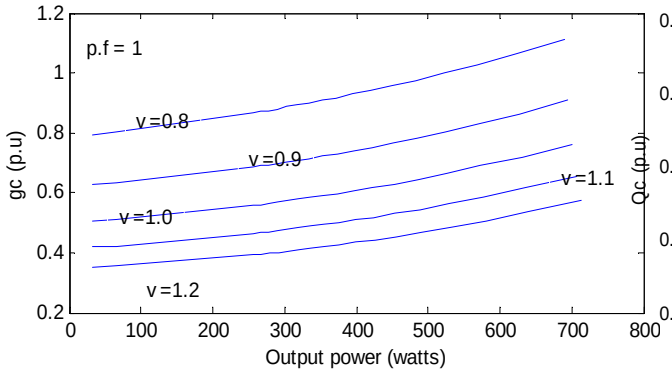

Fig. 11. g_c required at different loads to keep V_t is maintained constant at 1 p.u (with use PSO method)

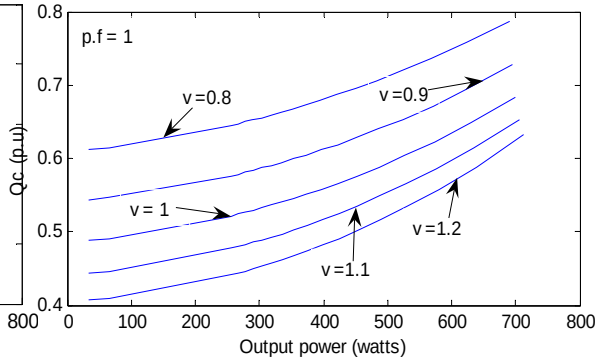

Fig. 12. VAR required at different loads to keep V_t is maintained constant at 1 p.u (with use PSO method)

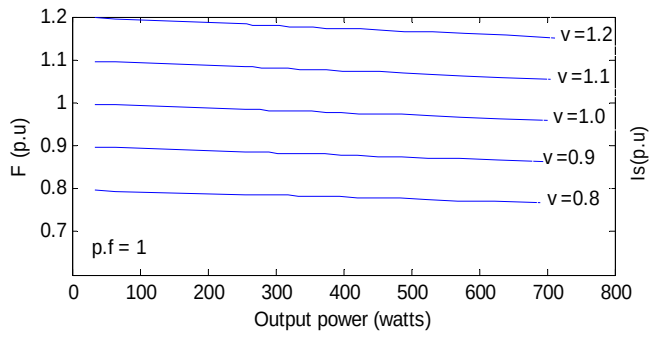

Fig. 13. Variation Freq. at different loads to keep V_t is maintained constant at 1 p.u (with use PSO method)

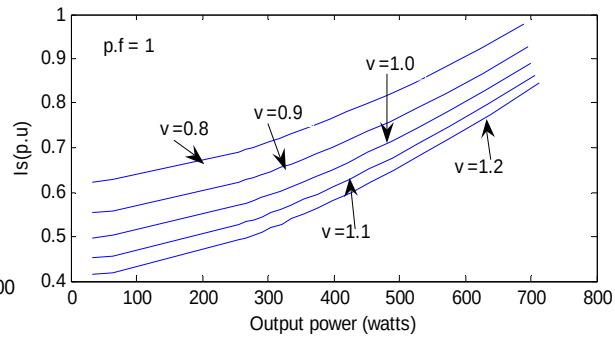

Fig. 14. Variation Is, at different loads to keep Vt is maintained constant at 1 p.u (with use PSO method)

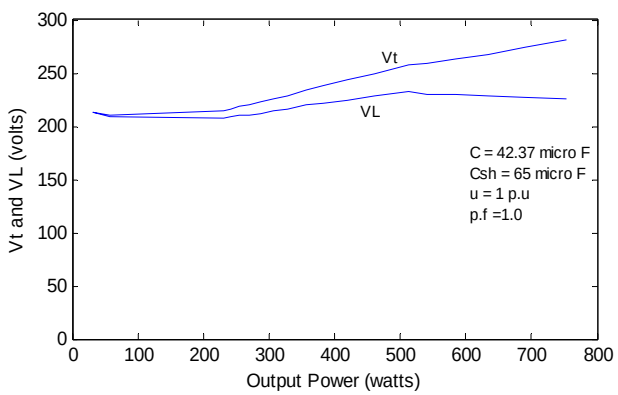

Fig. 15. Voltage char. of short-shunt SEIG at u. p.f load

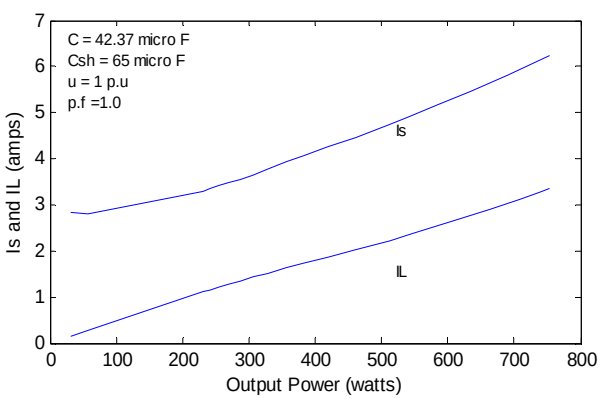

Fig. 16. Current char. of short-shunt SEIG at u. p.f load

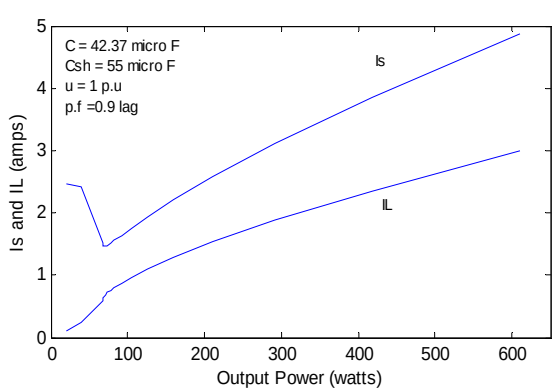

Fig. 17. Current char. of short-shunt SEIG at 0.9 p.f load

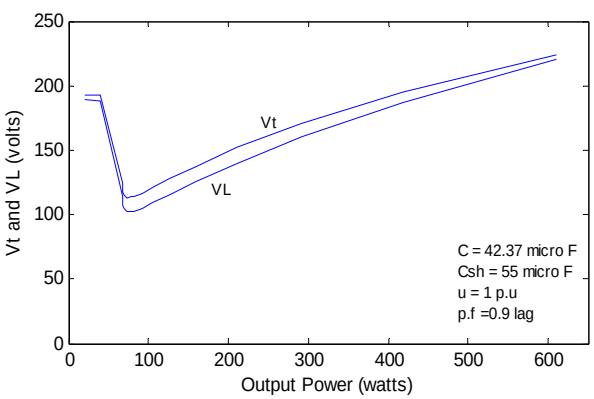

Fig. 18. Voltage char. of short-shunt SEIG at 0.9. p.f load

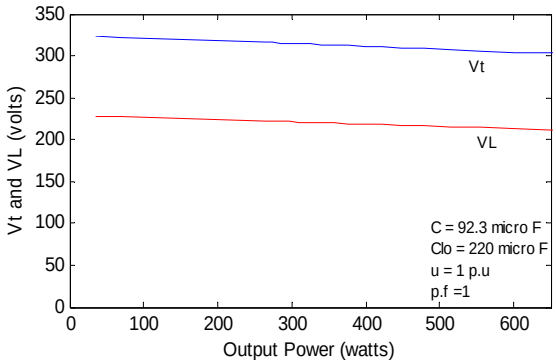

Fig. 19. Variation of terminal and load voltages of long-shunt SEIG at u.p.f load

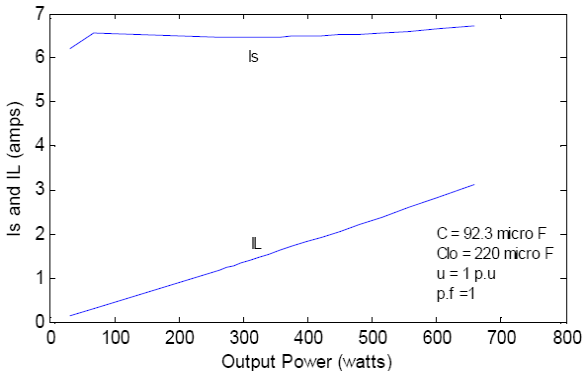

Fig. 20. Current char. of long-shunt SEIG at u.p.f load

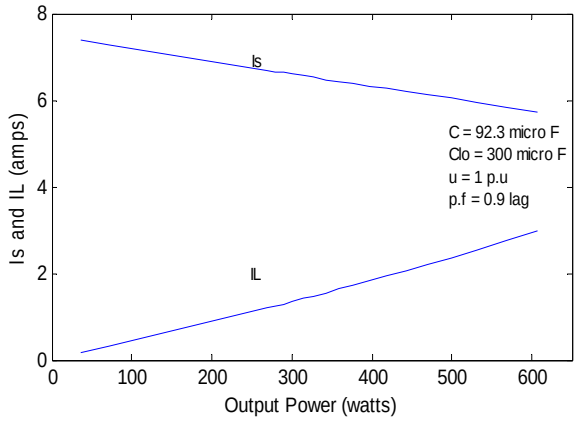

Fig. 21. Current char. of long-shunt SEIG at 0.9 p.f load

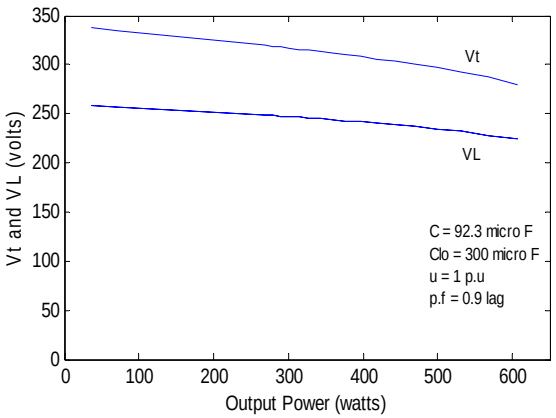

Fig. 22. Voltage char. of long-shunt SEIG at 0.9 p.f load

5.4 With long-shunt compensation

The steady state performance of long-shunt single phase SEIG is studied with upf and 0.9 pf load as shown in Figs. 19∼22. In long-shunt configuration, the short-shunt component Xcsh/F is neglected in z9. To find unknown values of X_M and F, the Eq. (9) is again solved by including the X_{clo}/F in z_5. With long-shunt compensation, it is observed that the voltage regulation with reactive load is better as compared to short-shunt. A comparative study of the results with PSO method and those are obtained with NR method[9] are depicted in Tab. 3.

From the Tab. 3, it is evident that the proposed method is efficient and robust. The results presented in Tab. 3 are for the variation of loads between 1.8 Ω and 40 Ω, for $X_C = 1.516\ p.u$ (56 μF) and $v = 1\ p.u$. It is observed that the time taken using PSO method is very less as compared to the NR method. The values X_M and F obtained using above are used to compute the performance of the single phase single winding SEIG under various conditions. Close agreement between the results obtained using two methods are observed. The main advantage of this method is that, there is no need of any initial guess values, which highly affects the performance and convergence criterion of the NR method.

Some times, wrong initial guesses in NR method will cause the divergence of the solution. The other advantage over NR method is that the proposed PSO method does not requires any tedious manual work involving calculations of partial differential equations and Jacobian matrix. Sometimes, calculation of Jacobian matrix is not possible if the matrix is symmetrical. Also the calculation of Jacobian matrix becomes cumbersome and time consuming as the number of variables and size of the Jacobian increases. Even to calculate unknown parameters X_C and F to maintain the constant terminal case, there is no need to formulate the equations once again in PSO method, and the analysis of SEIG with short shunt and/or long shunt can be easily carried out with this method in similar way.

6 Conclusion

The steady state performance of single phase single winding SEIG based on branch impedance method using graph theory (tie-set) and PSO with different compensation under various operating conditions has investigated in this paper. The effectiveness of additional series capacitance to provide additional VAR with load to improve and maintain constant terminal voltage and output power is presented. It is observed that similar characteristics obtained in both short and long shunt configuration. Thus, the investigation suggests a workable model of single phase single winding SEIG using PSO which is simple, rugged and stand alone self regulated capacity. Based on closed agreement between the results using NR method and PSO method at different loads, it can be concluded that the approach made in mathematical analysis is elegant.

References

[1] S. Alghuwainem. Steady-state analysis of a self-excited induction generator including transformer saturation. *IEEE Transactions on Energy Conversion*, 1999, **14**(3): 667–672.

[2] T. Chen, L. Lai. A novel single-phase self regulated self-excited induction generator using a three-phase machine. *IEEE Transactions on Energy Conversion*, 2001, **16**(2): 204–208.

[3] J. Kennedy, R. Eberhart. Particle Swarm Optimization. **in:** *IEEE International Conference on Neural Networks IV*, 4, Piscataway, NJ, 1995, 1942–1948.

[4] H. Rai, B. Singh. Investigation on single-phase self -excited induction generator for stand by power generation. **in:** *Proceedings of 32nd Intersociety Conference on Energy Conversion Engineering*, 3, 1997, 1996–2000.

[5] Y. Shi, R. Eberhart. A modified Particle Swarm Optimizer. **in:** *IEEE International Conference on Evolutionary Computation*, Piscataway, NJ, 1998, 67–73.

[6] B. Singh, L. Shridhar, C. Jha. Improvement in the performance of self-excited induction generator through series compensation. *IEE Proceedings-Generation, Transmission and Distribution*, 1999, **146**(6): 602–608.

[7] G. Singh. Self-excited induction generator research-a survey. *Electric power system research*, 2004, (69): 107–114.

[8] S. singh, M. Jain. Steady state analysis of a self excited induction generator with an AC-DC conversion scheme for small scale generation. *Electrical Power System Research*, 1991, **20**: 95–104.

[9] S. Velusami, S. Singaravelu. Steady state modeling and fuzzy logic based analysis of wind driven single phase induction generators. *Renewable Energy*, 2007, (32): 2386–2406.

Appendix

The machine has the following particulars: Single-phase, 4-ploe, 50 Hz, 225 V, 6 A, 750 W, 1500 rpm capacitor start Induction machine.

$$\text{Base voltage/current} = 225V/6A,\ \text{base power} = 1350W,\ R_m = 2.812\Omega,$$
$$R_r = 3.973\Omega,\ X_{lm} = X_{lr} = 6.410\Omega,\ v = 1p.u,\ \text{Load} = 33.75W - 750W.$$

The relationship between X_M and V_g/F is given by:

$$V_g/F = 1.689 - 0.2X_M \text{ (for } X_M < 3.2p.u) \text{ and } V_g/F = 2.844 - 0.55X_M \text{ (for } X_M > 3.2p.u).$$